


[View Journal Online](#)
[View Article Online](#)

Mononuclear pyrazine-2-carbohydrazone metal complexes: Synthesis, structural assessment, thermal, biological, and electrical conductivity studies

Ashish Bansod , Ravindra Bhaskar , Chandarshekhar Ladole , Nilesh Salunkhe ,
 Kanchan Thakare  and Anand Aswar *

Department of Chemistry, Sant Gadge Baba Amravati University, Amravati, 444602, India

* Corresponding author at: Department of Chemistry, Sant Gadge Baba Amravati University, Amravati, 444602, India.
 e-mail: aswaranand@gmail.com (A. Aswar).

RESEARCH ARTICLE

ABSTRACT



doi 10.5155/eurjchem.13.1.126-134.2186

Received: 17 September 2021
 Received in revised form: 15 November 2021
 Accepted: 12 February 2022
 Published online: 31 March 2022
 Printed: 31 March 2022

KEYWORDS

TGA
 Powder XRD
 Metal complexes
 Biological activity
 Electrical conductivity
 Pyrazinecarbohydrazone

Mononuclear complexes of VO(IV), Cr(III), Fe(III), MoO₂(VI), WO₂(VI), and UO₂(VI) with pyrazinecarbohydrazone ligand (*N'*-(1-(5-chloro-2-hydroxyphenyl)ethylidene)pyrazine-2-carbohydrazide) were synthesized and the prepared complexes were characterized by elemental analysis, magnetic susceptibility, powder X-ray analysis, various spectroscopic techniques (IR, ¹H NMR, ¹³C NMR, and Mass spectra), SEM, and thermal analysis. VO(IV) complex was additionally characterized by ESR study. The ligand behaves as a dibasic tridentate, coordinating through the phenolate oxygen, azomethine nitrogen, and enolate oxygen atoms towards the central metal ion. The analytical data suggest 1:1 metal to ligand stoichiometry for all complexes. The physicochemical data suggested octahedral geometry to Cr(III), Fe(III), MoO₂(VI), WO₂(VI), and UO₂(VI) complexes while square pyramidal to VO(IV) complex. The SEM analysis indicated the presence of well-defined crystals free from any shadow of the metal ion on their external surface with particle sizes of greater than 10 μm. Various kinetics and thermodynamic parameters are calculated using Coats-Redfern method and on the basis of half decomposition temperature the thermal stability order of complexes was found to be Cr(III) < WO₂(VI) < Fe(III) < MoO₂(VI) < VO(IV) < UO₂(VI). The solid-state electrical conductivity of compounds was measured in their pellet form in the temperature range from 313-373 K. The conductivity data vary exponentially with the absolute temperature and obey Arrhenius equation indicating their semiconducting behavior. The antibacterial as well as antifungal activities of ligand and its metal complexes were evaluated *in vitro* against Gram positive bacteria (*S. aureus* and *B. subtilis*) and Gram-negative bacteria (*E. coli* and *S. typhi*) and fungal strains (*C. albicans* and *A. niger*). The activity data revealed metal complexes are found to be more active than the ligand.

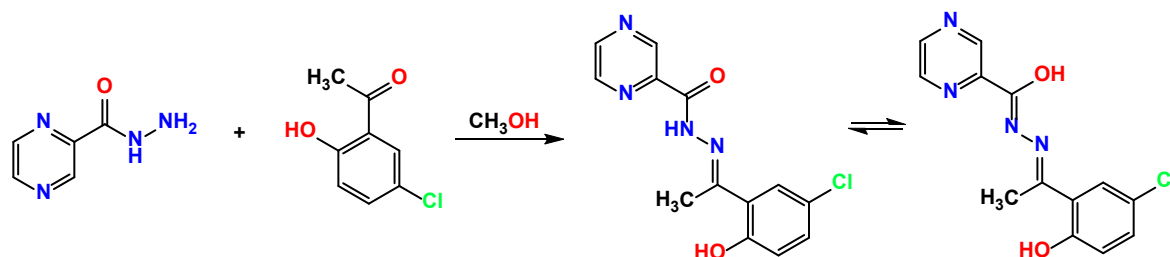
Cite this: *Eur. J. Chem.* 2022, 13(1), 126-134

Journal website: www.eurjchem.com

1. Introduction

The Schiff bases are widely studied ligands, in their neutral or deprotonated forms, to form stable complexes with most of the transition and non-transition metal ions. Schiff base hydrazones also show numerous physiological and biological applications such as insecticides, herbicides, rodenticides, tuberculosis, nematocides, plant growth regulators, antibacterial, antiviral, antifungal, antidepressant, antianalgesic, anticonvulsant, antimalarial, antitumoral, anti-HIV, antipsychotic, trypanocidal, anticoagulant, polymers initiators, antioxidants, plasticizers and stabilizers, and enzymatic inhibitors [1-7]. Tridentate and tetradentate hydrazones are of particular interest not only for existing them in *keto-enol* forms and can coordinate in neutral, monoanionic, dianionic or trianionic forms but they also offer a variety of bonding possibilities in metal complexes which have even coordination number of six or seven. Furthermore, Schiff base hydrazones bearing nitrogen containing moiety have attracted considerable attention due to their impressive chemical and analytical applications as

selective metal extracting agent as well as in spectroscopic determination of certain transition metals [8,9]. Electrical conductivity is an important physical property of solids not only for practical applications, but also to interpret various physical phenomena. Moreover, numerous reports suggest that pyrazonic acid hydrazone and associated compounds containing heterocyclic moiety may exhibit wide variety of biological and pharmacological properties as well [10,11]. In order to establish a relationship between the chemical structure and biological activity, divalent metal complexes of hydrazones including heterocyclic moieties involving nitrogen, oxygen and sulphur as coordinating functionalities have been studied extensively, however, complexes of higher valent metal ions are still unexplored. Recently, we have reported the biologically active hydrazone Schiff base and its divalent metal complexes and their interesting electrical and biological properties prompted us to extend further our work with higher valent metal ion complexes of pyrazine carbohydrazone of 2-hydroxy-5-chloroacetophenone to see metalation effect on such properties compared to non-substituted analog [12,13].



Scheme 1. Synthesis and tautomeric forms of ligand, H₂L.

The literature survey revealed that no work has been carried out so far on the hydrazone derived from pyrazine-2-carbohydrazide and 1-(5-chloro-2-hydroxyphenyl)ethan-1-one and its complexes with higher valent ions. Hence, it was thought worth considering the investigation of this ligand towards higher valent metal complexes. Therefore, herein we have synthesized complexes of Cr(III), Fe(III), VO(IV), MoO₂(VI), WO₂(VI), and UO₂(VI) ions with the ligand, *N'*-(1-(5-chloro-2-hydroxyphenyl)ethylidene)pyrazine-2-carbohydrazide. The ligand and its complexes have been screened for *in vitro* antibacterial activity against Gram +ve bacteria (*S. aureus*, *B. subtilis*) and Gram -ve bacteria (*E. coli* and *S. typhi*) as well as fungal pathogenic strains (*C. albicans* and *A. niger*). Furthermore, the solid-state electrical conductivity of ligand and its complexes was also studied in the solid pellet form.

2. Experimental

2.1. Materials and physical measurements

Analytical reagent grade metal salts (Vanadylsulphate pentahydrate, chromiumchloride hexahydrate, anhydrous ferricchloride and uranyl nitrate hexahydrate of 99% purity, S.D. fine chemicals, India) were used as received. The ligand pyrazine-2-carbohydrazone of 2-hydroxy-5-chloroacetophenone, MoO₂(acac)₂ and WO₂(acac)₂ were prepared according to literature methods [14-16].

2.2. Instrumentation

The infrared spectra were recorded using KBr on a Shimadzu 8201 spectrophotometer in the range 400-4000 cm⁻¹. The carbon, hydrogen, and nitrogen analyses were carried out on a CarloErba 1108 elemental analyser. ¹H and ¹³C NMR spectra of the ligand were recorded on Bruker Advance II, 400 MHz, NMR spectrophotometer in DMSO-*d*₆ with TMS as an internal standard. Magnetic measurements were carried out by the Sherwood magnetic susceptibility balance MK-1 at room temperature. The solid-state diffuse reflectance spectra of the complexes were recorded in the 200-1200 nm range using MgO as diluent on a Cary 60 UV-Vis spectrophotometer. The X-band ESR spectrum of VO(IV) complex was recorded on Varian E-112 spectrometer using TCNE (tetracyanoethylene) as the g-marker. Thermal analysis of compounds was carried out on Perkin-Elmer TGA-4000 analyzer in the temperature range 40-750 °C in air atmosphere with a heating rate of 20 °C/min. Metal contents of the complexes were analyzed gravimetrically after decomposing the organic matter with a mixture of HClO₄, H₂SO₄ and HNO₃ (1:1.5:2.5) and then igniting to metal oxide. The chloride contents were determined as AgCl by following a standard procedure [17]. The solid-state electrical conductivity of the prepared complexes has been measured by using two probe techniques over a temperature range 313-373 K. The samples were in the form of a pellet having diameter 13mm and thickness of 2-3 mm at pressure of approximately 1×10⁸ Pa. The pellet was placed between two copper electrodes with silver

paste on both sides so that there may have good ohmic contact between pellet and electrodes. The temperature of sample was measured with the accuracy ±1 °C with a calibrated Ni-NiCr thermocouple inserted inside the cell. The activation energies of electrical conductance were calculated using equation $\sigma = \sigma^0 \exp(E_a/KT)$. X-ray diffraction patterns were obtained with a Bruker AXS, D8 advance equipped with Si(Li) PDS. Mass spectra were recorded on a Waters, Q-TOF micromass (LC-MS) spectrometer. The surface morphology was observed using a JEOL Model JSM-6390LV scanning electron microscope.

2.3. Synthesis

2.3.1. Synthesis of the ligand (H₂L)

A solution of pyrazine-2-carbohydrazide (1 g, 7.2 mmol) and 1-(5-chloro-2-hydroxyphenyl)ethan-1-one (1.24 g, 7.2 mmol) in methanol (30 mL) was refluxed in the presence of a catalytic amount of glacial acetic acid (1-2 drops) for ca. 4 h on a water bath. After completion of the reaction, methanol was distilled off using rotary evaporator to nearly half of its volume and then cooled to room temperature, which resulted in a lemon-yellow solid. This was filtered, washed with hot ethanol and crystallized from DMF. The purity of the compound was checked by TLC (Scheme 1).

N'-(1-(5-Chloro-2-hydroxyphenyl) ethylidene)pyrazine-2-carbohydrazide (H₂L): Yield: 78%. M.p.: 248-250 °C. FR-IR (KBr, ν, cm⁻¹): 3336 (OH), 3162 (NH), 1672 (C=O), 1626 (C=N), 1294 (C-O). ¹H NMR (DMSO-*d*₆, 400 MHz, δ, ppm): 13.11 (s, 1H, OH), 11.60 (s, 1H, NH), 9.28 (s, 1H, *J* = 1.4 Hz, C3-H), 8.95 (d, 1H, *J* = 2.4 Hz, C6-H), 8.83 (dd, 1H, *J* = 1.5, 2.4 Hz, C5-H), 7.67 (d, *J* = 2.6 Hz, 1H, C6'-H), 7.36 (dd, 1H, *J* = 2.6, 8.8 Hz, C4'-H), 6.95 (d, 1H, *J* = 8.8 Hz, C3'-H), 2.51 (s, 3H, CH₃). ¹³C NMR (DMSO-*d*₆, 400 MHz, δ, ppm): 160.2 (C=N), 159.0 (C2'), 157.4 (C=O), 148.1 (C6), 144.1 (C3 and C5), 143.6 (C2), 131.2 (C4'), 128.0 (C6'), 122.3 (C5'), 119.1 (C3'), 120.7 (C1'), 14.1 (CH₃). MS (ESI, *m/z* (%)): 291.0622 (calc: 290.9100) [M+1].

2.3.2. Synthesis of VO(IV), Cr(III), Fe(III), and UO₂(VI) complexes

Metal complexes of VO(IV), Cr(III), Fe(III), and UO₂(VI) were prepared by following general method. An equimolar amount of ligand (H₂L) (2.91 g, 0.01 mol) and respective metal salt (0.01 mol) were dissolved separately in DCM and MeOH mixture (50:50, v:v) (25 mL). Both the solutions were mixed in warm conditions with continuous stirring. The reaction mixture was further refluxed for ca. 5 h on an oil bath. The pH of the reaction mixture was adjusted ca. 7.0 by adding methanolic solution of sodium acetate (0.5 g) and refluxing further continued for another 1 h. The reaction mixture was cooled to room temperature the precipitate separated out was filtered, washed with cold DCM, methanol, and petroleum ether and finally dried under vacuum over CaCl₂.

Table 1. Physicochemical and conductivity data of ligand and its metal complexes.

Compound	Color	Empirical formula	Elemental analysis, Found (Calcd.), %					Solid state electrical conductance	
			C	H	N	Cl	M	σ^*	E_a (eV)
H ₂ L	Reddish lemon	C ₁₃ H ₁₁ Cl ₁ N ₄ O ₂	52.98 (53.71)	4.14 (3.81)	18.98 (19.27)	12.00 (12.19)	-	4.17×10 ⁻¹³ 3.80×10 ⁻¹¹	0.440
[Cr(L)(Cl)(H ₂ O) ₂]	Deep scarlet	C ₁₃ H ₁₃ Cl ₂ N ₄ O ₄ Cr ₁	37.18 (37.88)	3.01 (3.18)	13.29 (13.59)	17.15 (17.20)	12.46 (12.62)	1.52×10 ⁻¹² 9.64×10 ⁻¹¹	0.755
[Fe(L)(Cl)(H ₂ O) ₂]	Dark amber	C ₁₃ H ₁₃ Cl ₂ N ₄ O ₄ Fe ₁	32.86 (37.53)	2.89 (3.15)	13.25 (13.47)	17.02 (17.04)	13.27 (13.42)	7.44×10 ⁻¹¹ 2.36×10 ⁻⁹	0.738
[VO(L)(H ₂ O)]	Chartreuse	C ₁₃ H ₁₁ Cl ₁ N ₄ O ₄ V ₁	41.40 (41.79)	2.65 (2.97)	14.70 (14.99)	9.40 (9.49)	13.32 (13.63)	6.13×10 ⁻¹² 8.83×10 ⁻¹⁰	0.929
[MoO ₂ (L)(H ₂ O)]	Mustard	C ₁₃ H ₁₁ Cl ₁ N ₄ O ₅ Mo ₁	36.97 (35.92)	2.38 (2.55)	13.06 (12.89)	8.10 (8.16)	22.49 (22.08)	7.42×10 ⁻¹¹ 5.86×10 ⁻⁹	0.846
[WO ₂ (L)(H ₂ O)]	Avocado	C ₁₃ H ₁₁ Cl ₁ N ₄ O ₅ W ₁	29.21 (29.88)	2.03 (2.12)	10.38 (10.72)	6.75 (6.78)	35.05 (35.18)	6.24×10 ⁻¹² 3.72×10 ⁻¹⁰	0.553
[UO ₂ (L)(CH ₃ OH)]	Terracotta	C ₁₄ H ₁₃ Cl ₁ N ₄ O ₅ U ₁	21.96 (28.46)	2.07 (2.22)	9.16 (9.48)	5.95 (6.00)	40.19 (40.29)	5.37×10 ⁻¹² 3.55×10 ⁻¹⁰	0.518

* $\Omega^{-1}\text{cm}^{-1}$, at 313 and 373 K.**Table 2.** Infrared spectral bands (cm^{-1}) of the ligand and its metal complexes

Compound	$\nu(\text{OH-N})$	$\nu(\text{NH})$	$\nu(\text{C=O})$	$\nu(\text{C=N})$	$\nu(\text{C-O})$ phenolic	$\nu(\text{C-O})$ enolic	$\nu(\text{N-N})$	$\nu(\text{M-O})$	$\nu(\text{M-N})$
H ₂ L	3336	3162	1672	1626	1294	-	968	-	-
[VO(L)(H ₂ O)]	-	-	-	1612	1320	1244	982	554	421
[Cr(L)(Cl)(H ₂ O) ₂]	-	-	-	1618	1330	1270	995	506	426
[Fe(L)(Cl)(H ₂ O) ₂]	-	-	-	1614	1306	1265	996	510	429
[MoO ₂ (L)(H ₂ O)]	-	-	-	1615	1318	1248	982	512	418
[WO ₂ (L)(H ₂ O)]	-	-	-	1610	1314	1246	994	522	412
[UO ₂ (L)(CH ₃ OH)]	-	-	-	1604	1324	1258	998	548	428

2.3.3. Synthesis of MoO₂ and WO₂ complexes

A hot methanolic solution (25 mL) of MoO₂(acac)₂ (0.44 g, 1 mmol) was mixed in dropwise with a hot methanolic solution of ligand (H₂L) (2.91 g, 0.1 mmol) with vigorous shaking. The resulting turbid solution was filtered and then refluxed on a water bath with continuous stirring for ca 4 h. After reducing volume of the solution to ca. 10 mL and cooling at 10 °C overnight, the separated colored product obtained was filtered, washed with methanol followed by petroleum ether and finally dried in desiccator over anhydrous CaCl₂. The WO₂ complex was prepared under similar conditions as above using WO₂(acac)₂ and H₂L.

2.4. Antimicrobial activity

The antimicrobial activities of the ligand and its complexes were carried out at Department of Microbiology, Shri Shivaji College, Akola by disc diffusion method against *S. aureus* (MTCC 96), *B. subtilis* (MTCC 8979) as Gram positive bacteria and *E. coli* (MTCC 443), and *S. typhi* (MTCC 442) as Gram-negative and as well as fungi, *C. albicans* (MTCC 227) and *A. niger* (MTCC 282) at 1.0 mg/mL using disc diffusion method and studied the zone of inhibition after 24 h of incubation period [18]. The ciprofloxacin and clotrimazole were used as standard drugs for antibacterial and antifungal activity. Minimum inhibitory concentration (MIC) of the compounds against test organisms was determined by the broth micro dilution method. All these tests were performed in triplicates under identical conditions and DMSO used as a negative control and model values were selected. Activity was determined by measuring the diameter of the zone showing complete inhibition and has been expressed in mm.

3. Results and discussion

The reaction between pyrazine-2-carbohydrazide and 1-(5-chloro-2-hydroxyphenyl) ethan-1-one in methanol yields a hydrazone ligand. The formation of ligand was confirmed by elemental and spectral data. All complexes are colored solids, air stable at room temperature and insoluble in common solvents such as ethanol, methanol, chloroform, benzene, cyclohexane, acetone, diethyl ether and but sparingly soluble in DMF and DMSO. The analytical and physical data of the metal

complexes are summarized in Table 1. The elemental analysis data confirm the molecular formula and 1:1 metal:ligand stoichiometry of complexes. The mass spectrum of the ligand showed a molecular ion peak at m/z 291 which is consistent with its formula weigh. The ¹H NMR spectrum of ligand exhibits two resonances at δ 11.60 and 13.11 ppm (singlet, ¹H each) due to NH and phenolic protons, respectively. A sharp signal observed at δ 2.51 ppm due to the methyl protons of the hydroxyl acetophenone moiety indicates the formation of ligands. The insufficient solubility of the complexes, even in DMSO-*d*₆ has prevented us from carrying out ¹H NMR and UV-Visible solution studies of complexes.

3.1. IR spectra

IR spectra of complexes are compared with that of the free ligand to find out the points of attachment of the ligand to the metal ions in their complexes and assigning the coordination mode. The important IR bands are summarized in Table 2. IR spectrum of the ligand shows a medium intensity band at 3336 cm^{-1} due to intramolecular hydrogen bonded hydroxyl group $\nu(\text{O-H}\cdots\text{N})$ [19]. This band has been disappeared in the spectra of complexes indicated the deprotonation of the phenolic proton, followed by coordination of phenolate oxygen atom with the metal atoms. This is further supported by the upward shifting of $\nu(\text{C-O})$ phenolic frequency in the spectra of complexes by 12-36 cm^{-1} from 1294 cm^{-1} attributed the participation of phenolic oxygen in complexation [20]. The ligand exhibits a strong band at 1626 cm^{-1} due to $\nu(\text{C=N})$ (azomethine) and this band has been shifted to lower frequencies in complexes by 8-22 cm^{-1} , indicating donation of the lone pair of electrons on azomethine nitrogen to metal center, this has been strengthened by the upward shift of $\nu(\text{N-N})$ band from 968 to 982-998 cm^{-1} in the spectra of complexes also supported the coordination of the azomethine nitrogen atom to metal [21]. The high frequency shift of the $\nu(\text{N-N})$ band is expected because of the diminished repulsion between the lone pairs of adjacent nitrogen atoms as a result of coordination via azomethine nitrogen [22]. The IR spectrum of the ligand shows a strong band at 3162 and 1672 cm^{-1} due to N-H and C=O groups, respectively. The absence of these bands in the spectra of complexes indicates the destruction of carbonyl moiety as a result of the enolization and subsequent coordination of the enolate oxygen to metal [23].

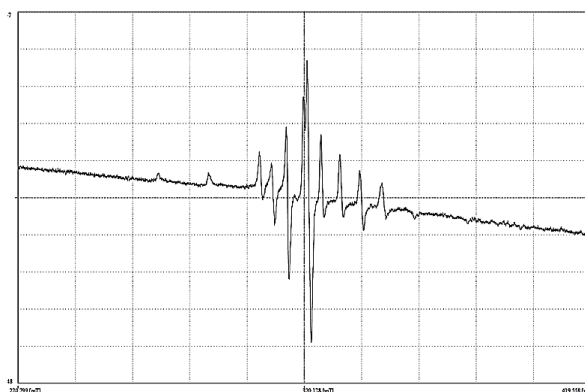


Figure 1. ESR spectrum of [VO(L)(H₂O)] complex.

The appearance of new medium intensity band in the region 1244-1270 cm⁻¹ in the spectra of complexes due to coordination of enolic oxygen after deprotonation. The oxovanadium (IV) complex exhibits an additional band at ~982 cm⁻¹ which may be assigned due to $\nu(\text{V}=\text{O})$ [24]. The [UO₂(L)(CH₃OH)] complex shows $\nu_{\text{sym}}(\text{O}=\text{U}=\text{O})$ and $\nu_{\text{asy}}(\text{O}=\text{U}=\text{O})$ stretches at 810 and 910 cm⁻¹, respectively, observed in normal ranges for the most of the dioxouranium (VI) complexes [25].

The force constant ($F_{\text{U-O}}$) value obtained for the complex is 6.65 m.dynes/Å while bond length was found to be 1.73 Å [26]. The coordination of methanol to uranium ion is further confirmed by the appearance of a new band at 1005 cm⁻¹ in UO₂(VI) complex, the $\nu(\text{C}-\text{O})$ stretch in methanol appears at 1034 cm⁻¹. Dioxomolybdenum (VI) complex shows bands at 866 cm⁻¹ due to symmetric and at 925 cm⁻¹ due to asymmetric stretching frequency of *cis*-MoO₂. Using McGlynn and Jones method, the $F_{\text{Mo-O}}$ and $R_{\text{Mo-O}}$ are calculated and are found to be 6.91 m.dynes/Å and 1.73 Å, respectively [27,28]. The presence of a *cis*-WO₂ moiety in the complex WO₂(VI) may be inferred from the appearance of two bands in the region 906-925 cm⁻¹ [29].

All complexes show a broad band in the 3372-3444 cm⁻¹ region, which may be due to coordinated water/methanol [30]. This band was followed by another non-ligand band at *ca* 1560-1592 and 848-884 cm⁻¹ confirmed the presence of coordinated water molecule/methanol. Appearance of new weak intensity non-ligand bands in the region 506-554 and 412-429 cm⁻¹ in all complexes are assigned to $\nu(\text{M}-\text{O})$ and $\nu(\text{M}-\text{N})$ stretching vibrations, respectively [31]. The IR spectral data and valence requirement of the metal ion suggest the dibasictridentate behavior of the ligand coordinating through the phenolic oxygen, azomethine nitrogen and enolic oxygen atoms.

3.2. Electronic spectra and magnetic moments

The reflectance spectrum of Cr(III) complex exhibits three bands at 595, 415, and 262 nm due to ${}^4\text{A}_{2g}(\text{F}) \rightarrow {}^4\text{T}_{2g}(\text{F})$, ${}^4\text{A}_{2g}(\text{F}) \rightarrow {}^4\text{T}_{1g}(\text{F})$ and ${}^4\text{A}_{2g}(\text{F}) \rightarrow {}^4\text{T}_{1g}(\text{P})$, transitions, respectively, suggesting an octahedral environment around the chromium ion [32]. The ν_2/ν_1 ratio is found to be 1.36 which is very close to the value of 1.42 obtained for pure octahedral Cr(III) complexes [33]. The calculated values of crystal field parameters Dq (1718 cm⁻¹), B (689 cm⁻¹), β (0.71 cm⁻¹) are also in good agreement with those reported for an octahedral Cr(III) complexes [34]. The complex shows the lower value of B than that of the free ion which indicates the orbital overlapping, delocalization of the d -orbital. Furthermore, this is well supported by its magnetic moment 3.91 B.M. indicating a d^3 configuration three unpaired electrons in the complex in consistent with an octahedral geometry [35]. The Fe(III) complex shows three bands at 850, 592 and 474 nm assignable

to ${}^6\text{A}_{1g} \rightarrow {}^4\text{T}_{1g}(\text{G})$, ${}^6\text{A}_{1g} \rightarrow {}^4\text{T}_{2g}(\text{G})$ and ${}^6\text{A}_{1g} \rightarrow {}^4\text{E}_g(\text{D})$, transitions, respectively, indicating octahedral geometry around metal ion [36]. The magnetic moment value is 5.89 B.M., which is indicative of octahedral geometry around Fe(III)ion [37]. The oxovanadium complex shows three bands at 769, 610 and 465 nm due to ${}^2\text{B}_2 \rightarrow {}^2\text{E}$, ${}^2\text{B}_2 \rightarrow {}^2\text{B}_1$ and ${}^2\text{B}_2 \rightarrow {}^2\text{A}_1$, transitions, respectively. The fourth band appears at 345 nm which may be due to the charge transfer transition, indicating a square pyramidal coordination around vanadium ion [38]. The magnetic moment is 1.78 B.M. which is also close to the spin only value for one unpaired electron. The dioxouranium UO₂(VI) complex shows a weak band at 447 nm which is assign to the ${}^1\Sigma_g^+ \rightarrow {}^3\Pi_u$ transition [39]. The MoO₂(VI) and WO₂(VI) complexes exhibit one band about at ~417 nm due to metal to ligand charge transfer transition between the lowest empty d -orbital of the metal and the highest occupied ligand orbital [40]. The MoO₂(VI), UO₂(VI), and WO₂(VI) complexes are found to be diamagnetic as expected for their electronic configurations and most likely to be an octahedral geometry around metal ions.

3.3. ESR spectra

As we could not get a suitable single crystal, the liquid nitrogen temperature ESR spectrum of VO(IV) complex gave typical eight-line pattern (Figure 1) similar to those reported for mononuclear vanadium molecule. The spectrum of the vanadium complex is somewhat resolved due to hyperfine coupling with vanadium nucleus. The spectrum is interpreted in terms of an effective spin of $1/2$. In this spectrum, EPR parameters g_{\parallel} and g_{\perp} were used to evaluate the geometry of the complex. In general, value of Lande factor also called 'g' factor, and for a free electron value is 2.00232. The various parameters were calculated from the spectrum and values are found to be $g_{\parallel} = 1.91$, $g_{\perp} = 1.98$, $g_{\text{av}} = 1.95$, $A_{\parallel} = 180$, $A_{\perp} = 73$ and $A_{\text{av}} = 108$, respectively. The $g_{\parallel} = 1.91$ and $g_{\perp} = 1.98$ and $g_{\text{av}} = 1.95$ values obtained for the VO(IV) complex are in agreement with those generally observed for a vanadyl complex with a square pyramidal disposition [41]. The g_{\parallel} values (< 2.3) support the covalent character of the metal-ligand bond in the complexes. The trend $g_{\parallel} < g_{\perp}$ and $A_{\parallel} > A_{\perp}$ in the complex indicated that the unpaired electron is localized in the d_{xy} orbital and the spectral features are characteristic of an axially compressed d^1_{xy} configuration for vanadyl complexes [42,43]. The covalent nature can also be ascertained from the spin-orbit coupling constant λ which is calculated using the equation $g_{\text{av}} = 2.0 [1 - (2\lambda/10Dq)]$, the g_{av} value is obtained from the relation, $g_{\text{av}} = 1/3 (g_{\parallel} + 2 g_{\perp})$ and $10Dq$ from the electronic spectrum. The lower value of λ (ca. 156 cm⁻¹) compared with that of free vanadyl ion (170 cm⁻¹) suggests considerable orbital overlap.

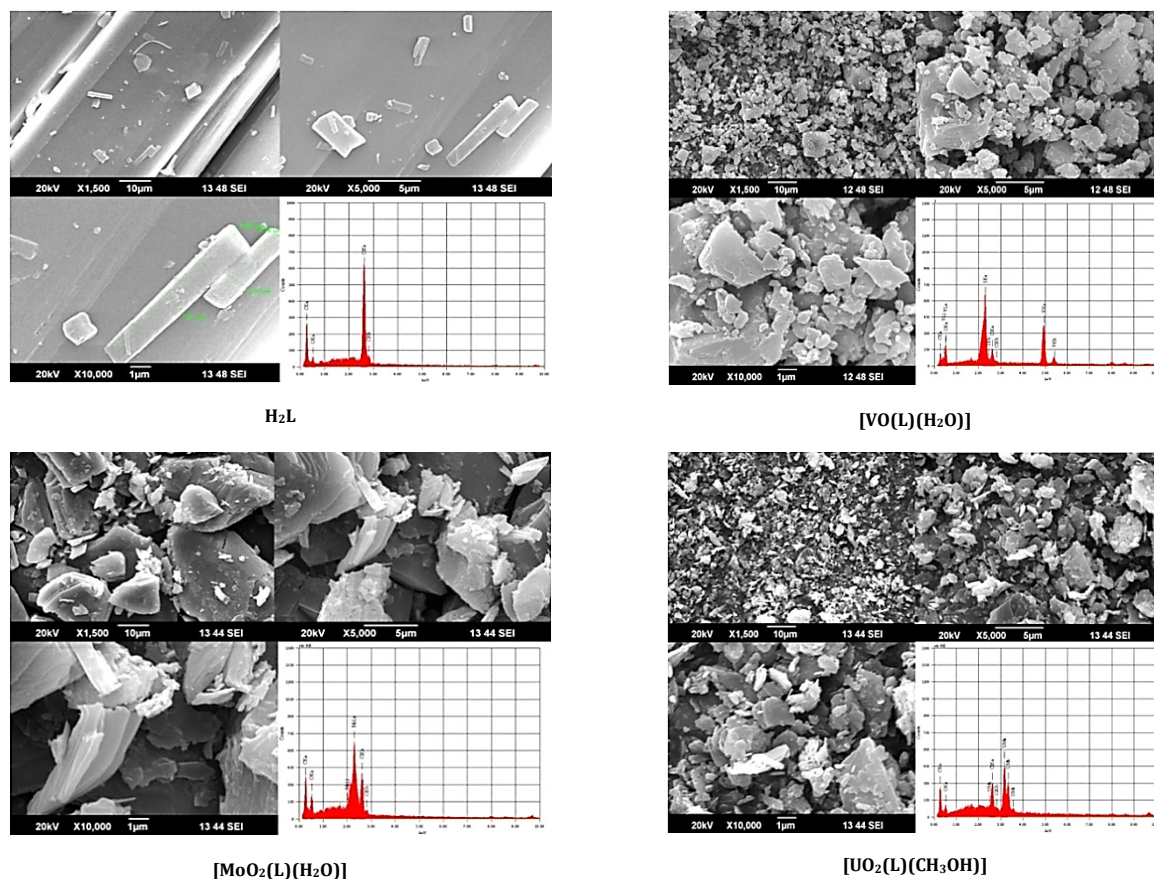


Figure 2. Scanning electron microscope image of investigated compound.

3.4. X-Ray powder diffraction and SEM analyses

The attempt to growing single crystal of the complexes is proved futile so far. Therefore, X-ray powder diffraction analysis of ligand and its $[MoO_2(L)(H_2O)]$ and $[UO_2(L)(CH_3OH)]$ complexes were recorded as representatives cases. Comparing the X-ray diffraction patterns of the ligand with its corresponding metal complexes indicate that the inter-planar spacing and the relative intensities are different, which could be attributed to the complex formation. It is found that the ligand and both complexes have triclinic structure with almost same configurations. Moreover, using the diffraction data, the mean crystallite sizes of the compounds, were calculated according to the Scherer's formula [44]. The crystal lattice parameters of H_2L ligand are $a = 16.5000 \text{ \AA}$, $b = 7.0800 \text{ \AA}$, $c = 4.8000 \text{ \AA}$, $\alpha = 99.470^\circ$, $\beta = 90.390^\circ$, $\gamma = 98.600^\circ$, $V = 546.59 \text{ \AA}^3$ belongs to triclinic system, for $[MoO_2(L)(H_2O)]$ complex are $a = 11.0800 \text{ \AA}$, $b = 13.2700 \text{ \AA}$, $c = 10.6800 \text{ \AA}$, $\alpha = 113.500^\circ$, $\beta = 104.980^\circ$, $\gamma = 91.105^\circ$, $V = 1377.79 \text{ \AA}^3$ and for $[UO_2(L)(CH_3OH)]$ complex are $a = 8.4418 \text{ \AA}$, $b = 6.200 \text{ \AA}$, $c = 10.8470 \text{ \AA}$, $\alpha = 90.880^\circ$, $\beta = 107.240^\circ$, $\gamma = 98.70^\circ$, $V = 610.318 \text{ \AA}^3$. The average crystallite particle size of the H_2L ligand, $[MoO_2(L)(H_2O)]$ and $[UO_2(L)(CH_3OH)]$ complexes were found to 24-44 nm and these values, indicating that the compounds are in nanocrystalline phase [45]. A comparison of values reveals that there is a good agreement between the calculated and observed values of $\text{Sin}^2\theta$. Some of the extra peaks present in the complexes compared to ligand suggest the coordination of the metal ion [46]. The microbial effect of the metal complexes may change their morphological profiles due to membrane integrity and cell wall of bacterial species. Thus, SEM studies may be linked with the interaction of chemicals with those of bacterial inhibition. SEM images of the ligand and its $VO(IV)$, $MoO_2(VI)$, and $UO_2(VI)$ complexes were

recorded to check the surface morphology of the ligand and its complexes. The micrograph of the ligand and its complexes are presented in Figure 2. The micrographs indicated the presence of well-defined crystals free from any shadow of the metal ion on their external surface with particle sizes of greater than 10 μm. The average crystalline size shows that the particles were agglomerated and these complexes are polycrystalline with nanosized grains. Thus, the results obtained from SEM are in good agreement with the powder XRD results. The results of the energy dispersive X-ray analysis (EDS) plot inserted within each figure show the presence of metal peak in respective complex and the estimated value matches with the metal content obtained in the experimental section.

3.5. Thermal analysis

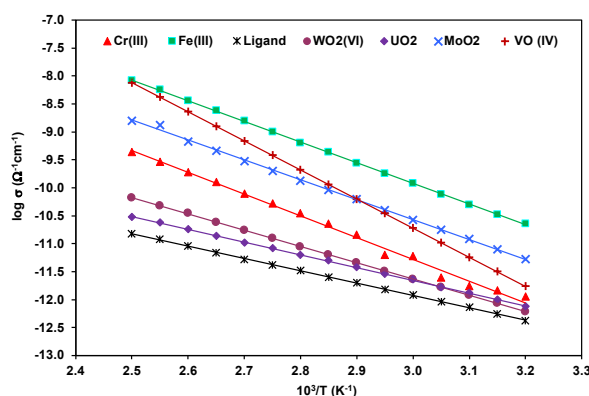
Thermal analyses of the ligand and its metal complexes were carried out in the temperature range from 40 to 750 °C with a heating rate of 10 °C/min in air atmosphere to examine their thermal stability and to investigate the percentage mass loss of compounds. The ligand decomposes in one step with continuous weight loss with increasing temperature with almost no residue at the end. A close look at the thermograms of the complexes indicated that they are thermally stable up to ca. 100 °C. The $Cr(III)$, $WO_2(VI)$, and $UO_2(VI)$ complexes decomposes in two stages whereas $VO(IV)$, $Fe(III)$, and $MoO_2(VI)$ complexes exhibits three overlapping steps decomposition pattern on increasing the temperature. In the first stage, loss of coordinated water /chloride/methanol molecule(s) takes place in the temperature range 130-180 °C. In all complexes, a rapid mass loss was observed between 270-410 °C due to partial elimination of ligand followed by a gradual mass loss up to 700 °C due to complete decomposition of organic moieties coordi-

Table 3. Kinetic and thermodynamic data of complexes.

Compound	Half decomp. temperature (°C)	Activation energy E_a (kJ/mol)	Frequency factor, Z (1/s)	Entropy change ΔS^* (J/mol.K)	Free energy ΔG^* (kJ/mol)
[VO(L)(H ₂ O)]	382	19.49	4.31×10^{-3}	-258.06	178.97
[Cr(L)(Cl)(H ₂ O) ₂]	325	18.77	4.41×10^{-2}	-237.87	160.64
[Fe(L)(Cl)(H ₂ O) ₂]	345	18.48	6.51×10^{-3}	-256.34	212.79
[MoO ₂ (L)(H ₂ O)]	380	19.37	2.03×10^{-2}	-246.37	160.54
[WO ₂ (L)(H ₂ O)]	340	17.44	1.65×10^{-2}	-246.70	166.20
[UO ₂ (L)(CH ₃ OH)]	440	16.60	4.63×10^{-3}	-257.36	259.01

Table 4. Zones of inhibition (mm) of growth of microorganisms.

Compounds	<i>S. aureus</i>	<i>B. subtilis</i>	<i>E. coli</i>	<i>S. typhi</i>	<i>A. niger</i>	<i>C. albicans</i>
H ₂ L	12	11	11	12	12	10
[VO(L)(H ₂ O)]	20	19	15	16	20	22
[Cr(L)(Cl)(H ₂ O) ₂]	15	16	14	15	18	17
[Fe(L)(Cl)(H ₂ O) ₂]	15	17	15	14	19	17
[MoO ₂ (L)(H ₂ O)]	19	20	16	17	21	19
[WO ₂ (L)(H ₂ O)]	16	15	14	15	17	18
[UO ₂ (L)(CH ₃ OH)]	15	17	15	14	18	18
Ciprofloxacin	23	25	22	22	-	-
Clotrimazole	-	-	-	-	22	22

**Figure 3.** Temperature dependence of log σ .

nated to metal ion. This mass loss may be due to oxidative degradation of complexes leading to formation of respective metal oxide as final product (i.e. V₂O₅, Cr₂O₃, Fe₂O₃, MoO₃, WO₃, and U₃O₈). The thermal stability of the metal complexes is higher than that of the free ligand. This may be due to that in all complexes five/six membered chelated rings and the M–N and M–O bonds are highly polarized [47]. The analysis of thermograms give further support to the composition and structure of the complexes proposed on the basis of elemental and other spectral studies.

The kinetic evaluation of the thermal decomposition of complexes were carried out and various thermodynamic parameters such as energy of activation (E_a), frequency factor (Z), free energy change (ΔG^*) and entropy of activation (ΔS^*) were evaluated by using Coats-Redfern method [48] and values are summarized in Table 3. The activation energy of decomposition was found in the range 16.60-19.49 kJ/mol. The thermal stability order on the basis of half decomposition temperature (Table 4) is found to be: Cr(III) < WO₂(VI) < Fe(III) < MoO₂(VI) < VO(IV) < UO₂(VI) (Table 3).

The observed high values of the activation energy of complexes may be due to the higher stability of the complexes due to their coordinated bond and it further suggested predicting the bond strength of ligand towards the metal ions. Higher value of E_a and lower values of Z favors the reaction to proceed slower than normal. The negative value of ΔS^* indicates that the activated complex has a highly ordered or more rigid structure than that of either the reactants or intermediate and that the reactions are slower than normal [49]. The similarity in the values of kinetic parameters indicates

a common decomposition mode in all compounds besides showing first order kinetics.

3.6. Solid state conductivity

The electrical conductivity (σ) was measured as a function of temperature (T) in the temperature range of 313-373 K and values are given in Table 1. Figure 3 show that electrical conductivity of complexes increases with increasing the temperature and decreases upon cooling over the studied temperature range, and this indicates their semiconducting behavior [50]. The general behavior of electrical conductivity follows the Arrhenius relation $\sigma = \sigma^0 \exp(E_a/KT)$, where σ^0 is a constant, E_a is the activation energy of electrical conduction, T is the absolute temperature and K is Boltzman constant. The conductivity of the free ligand is increased on complex formation with transition metal ions. This behavior is attributed to the inclusion of various metal cations in the π -electron delocalization of the ligand. The observed electrical conductivity value of the compounds at 373 K lies in the range 2.36×10^{-9} to $9.64 \times 10^{-11} \Omega^{-1} \text{cm}^{-1}$ and decreases in the order: Fe(III) > MoO₂(VI) > UO₂(VI) > WO₂(VI) > VO(IV) > H₂L > Cr(III) and activation energy in the range 0.440-0.929 eV and increases in the order: H₂L < UO₂(VI) < WO₂(VI) < Fe(III) < Cr(III) < MoO₂(VI) < VO(IV). The observed low value of electrical conductivity of compounds may be attributed to low molecular weight of complex due to which the extent of conjugation becomes low or undesirable morphology due to pressing of the sample into hard brittle pellet form [51].

3.7. Antimicrobial activity

The *in vitro* antimicrobial activity of ligand and its VO(IV), Cr(III), Fe(III), MoO₂(VI), WO₂(VI), and UO₂(VI) complexes was carried out and results are presented in Table 4. A comparative study of ligand and its metal complexes showed that the metal complexes exhibit higher activity. It is also observed from the data that the complexes are slightly more effective towards Gram +ve strains compared to the Gram -ve strains, though the level of action of a particular compound within the same type of bacteria is varying. This difference in activity probably may be attributed to the fact that the cell walls of Gram +ve bacteria have more antigenic properties as the outer lipid membrane is of polysaccharides. Although the complexes showed promising activities against the bacterial strains, however, their activities were found to be less than the standard ciprofloxacin (antibacterial drug) and clotrimazole (antifungal drug). The activity data shows the highest activity for VO(IV) complex very closed to standard drug ciprofloxacin followed by the MoO₂(VI) complex while others have no definite trend. Thus, the results indicate that the ligand and metal complexes exhibit good biological activity. The observed results are quite promising compared with the previous studies of non-substituted analog [12,13] and such better activity may be due to the presence of electron withdrawing Cl group at *para* position (H₂L) on aromatic ring in the structure. It has been suggested that the ligands with the N and O donor system might have inhibited enzymes production, since enzymes which require free hydroxyl groups for their activity appear to the especially susceptible to deactivation by the ions of the complexes [52].

The enhancement in biological activity on complexation of ligand with metal ions was explained by overtone's concept and Tweedy chelation theory [53,54]. According to Overtone's concept of cell permeability, the lipid membrane that surrounds the cell favors the passage of only the lipid-soluble materials, which makes the lipo solubility is an important factor which controls the antimicrobial activity. However, chelation reduces the polarity of the metal ion considerably because of the partial sharing of its positive charge with the donor groups and also due to delocalization of π -electron cloud on the whole chelating ring. This process, in turn, increases the lipophilic nature of the central metal atom, which favors its permeation more and efficiently through the lipid layer of cell membrane [55] thus destroying them more aggressively. However, chelation is not the only criterion for antimicrobial activity. Factors such as nature of metal ion, geometry of the complex, steric and pharmacokinetic factors, etc. also play an important role in deciding the antimicrobial potency of a compound. Apart from this, other factors such as solubility nature, conductivity, dipole moment, steric factor, and concentration influenced by the presence of metal ions may also be the possible reasons causing enhancement of the antimicrobial activity of the complexes as compared to free ligands.

4. Conclusions

In the present study, a heterocyclic hydrazone ligand was prepared by condensation of 1-(5-chloro-2-hydroxyphenyl) ethan-1-one with pyrazine-2-carbohydrazide and its metal complexes have been synthesized and characterized by various physicochemical and spectroscopic techniques. The octahedral geometry has been confirmed for Cr(III), Fe(III), MoO₂(VI), WO₂(VI), and UO₂(VI) complexes whereas the square pyramidal to VO(IV) complex. The ligand behaves dibasic tridentate coordinating through phenolate oxygen, azomethine nitrogen and enolate oxygen atoms. TG studies of the complexes also help to characterize the complexes. The TG analysis indicated that the complexes decompose in two or three overlapping steps whereas partially loss of organic part of the complexes take place though two overlapping steps; finally, they convert into

the corresponding metal oxide and various kinetic parameters have been evaluated by using Coats-Redfern method. The solid-state electrical conductivity of the compounds under studied temperature reflects their semiconducting behavior. The results of antimicrobial activity show that the metal complexes show enhanced inhibitory activity compared to the free ligand and under identical experimental conditions.

Acknowledgements

The authors are thankful to Sophisticated Analytical Instrument Facilities Centre, Cochin University, Kerala for providing Powder XRD, TG-DTA, SEM analysis. Authors are also thankful to Sophisticated Analytical Instrument Facilities Centre, Punjab University, Chandigarh for providing elemental analysis, IR and ¹H NMR and ¹³C NMR facility. Sant Gadge Baba Amravati University, Amravati (Maharashtra) for providing laboratory facilities is also gratefully acknowledged.

Disclosure statement

Conflict of interests: The authors declare that they have no conflict of interest. Ethical approval: All ethical guidelines have been adhered. Sample availability: Samples of the compounds are available from the author.

CRedit authorship contribution statement

Conceptualization: Anand Aswar; Methodology: Ravindra Bhaskar, Nilesh Salunkhe; Software: Ashish Bansod, Nilesh Salunkhe; Validation: Nilesh Salunkhe; Formal Analysis: Ashish Bansod; Investigation: Kanchan Thakare; Resources: Chandarshekhkar Ladole; Data Curation: Chandarshekhkar Ladole; Writing - Original Draft: Ashish Bansod; Writing - Review and Editing: Ashish Bansod; Visualization: Ashish Bansod; Funding acquisition: Ravindra Bhaskar; Supervision: Anand Aswar; Project Administration: Anand Aswar.

ORCID and Email

Ashish Bansod
 drashishbansod@gmail.com
 <https://orcid.org/0000-0001-9902-7198>
 Ravindra Bhaskar
 rsbhaskar61@gmail.com
 <https://orcid.org/0000-0001-5466-7765>
 Chandarshekhkar Ladole
 ladoleshekhkar2@gmail.com
 <https://orcid.org/0000-0002-8562-8563>
 Nilesh Salunkhe
 ngsalunkhe@gmail.com
 <https://orcid.org/0000-0001-7897-2721>
 Kanchan Thakare
 kanchaningole5@gmail.com
 <https://orcid.org/0000-0003-4333-2892>
 Anand Aswar
 aswaranand@gmail.com
 <https://orcid.org/0000-0003-4368-496X>

References

- [1]. Maurya, M. R. Probing the synthetic protocols and coordination chemistry of oxido-, dioxido-, oxidoperoxido-vanadium and related complexes of higher nuclearity. *Coord. Chem. Rev.* **2019**, *383*, 43–81.
- [2]. A-Ali Drea, A.; T. Mohammed, H. Simulation study of adrenaline synthesis from Phenylalanine. *J. Adv. Chem.* **2015**, *12*, 3888–3901.
- [3]. Ribeiro, N.; Galvão, A. M.; Gomes, C. S. B.; Ramos, H.; Pinheiro, R.; Saraiva, L.; Ntungwe, E.; Isca, V.; Rijo, P.; Cavaco, I.; Ramilo-Gomes, F.; Guedes, R. C.; Pessoa, J. C.; Correia, I. Naphthoylhydrazones: coordination to metal ions and biological screening. *New J. Chem.* **2019**, *43*, 17801–17818.
- [4]. Hossain, M. S.; Roy, P. K.; Zakaria, C. M.; Kudrat-E-Zahan, M. Selected Schiff base coordination complexes and their microbial application: A review. *Int. J. Chem. Stud.* **2018**, *6*, 19–31.
- [5]. Viswanathan, A.; Kute, D.; Musa, A.; Konda Mani, S.; Sipilä, V.; Emmert-Streib, F.; Zubkov, F. I.; Gurbanov, A. V.; Yli-Harja, O.; Kandhavelu, M. 2-(2-(2,4-dioxopentan-3-ylidene)hydrazinyl)benzimidazole as novel inhibitor of receptor tyrosine kinase and PI3K/AKT/mTOR signaling pathway in glioblastoma. *Eur. J. Med. Chem.* **2019**, *166*, 291–303.
- [6]. Martins, N. M. R.; Anbu, S.; Mahmudov, K. T.; Ravishankaran, R.; Guedes da Silva, M. F. C.; Martins, L. M. D. R. S.; Karande, A. A.; Pombeiro, A. J.

- L. DNA and BSA binding and cytotoxic properties of copper(II) and iron(III) complexes with arylhydrazone of ethyl 2-cyanoacetate or formazan ligands. *New J. Chem.* **2017**, *41*, 4076–4086.
- [7]. Le Goff, G.; Ouazzani, J. Natural hydrazone-containing compounds: Biosynthesis, isolation, biological activities and synthesis. *Bioorg. Med. Chem.* **2014**, *22*, 6529–6544.
- [8]. Yang, Y.; Gao, C.-Y.; Liu, J.; Dong, D. Recent developments in rhodamine salicylidene hydrazone chemosensors. *Anal. Methods* **2016**, *8*, 2863–2871.
- [9]. Mohanraj, M.; Ayyannan, G.; Raja, G.; Jayabalakrishnan, C. Evaluation of DNA binding, DNA cleavage, protein binding, radical scavenging and in vitro cytotoxic activities of ruthenium(II) complexes containing 2,4-dihydroxy benzylidene ligands. *Mater. Sci. Eng. C Mater. Biol. Appl.* **2016**, *69*, 1297–1306.
- [10]. Sebastian, O.; Thapa, A. Schiff base metal complexes of Ni, Pd and Cu. *J. Chem. Pharm. Res.* **2015**, *7* (10), 953–963. <https://www.iocpr.com/articles/schiff-base-metal-complexes-of-ni-pd-and-cu.pdf> (accessed February 10, 2022).
- [11]. Abd El-Halim, H. F.; Mohamed, G. G.; Khalil, E. A. M. Synthesis, spectral, thermal and biological studies of mixed ligand complexes with newly prepared Schiff base and 1,10-phenanthroline ligands. *J. Mol. Struct.* **2017**, *1146*, 153–163.
- [12]. Bhaskar, R. S.; Salunkhe, N. G.; Yaul, A. R.; Aswar, A. S. Synthesis, characterization, thermal behavior and biological studies of VOIV and MoO2 VI complexes of hydrazone ligand. *J. Indian Chem. Soc.* **2016**, *93*, 489–494.
- [13]. Bhaskar, R.; Salunkhe, N.; Yaul, A.; Aswar, A. Bivalent transition metal complexes of ONO donor hydrazone ligand: Synthesis, structural characterization and antimicrobial activity. *Spectrochim. Acta A Mol. Biomol. Spectrosc.* **2015**, *151*, 621–627.
- [14]. Synthesis, characterization and biological studies of some transition metal complexes with pyrazine Schiff base hydrazone ligand. *Jordan J. Chem.* **2020**, *15*, 61–72.
- [15]. Chen, G. J. J.; McDonald, J. W.; Newton, W. E. Synthesis of molybdenum (IV) and molybdenum(V) complexes using oxo abstraction by phosphines. Mechanistic implications. *Inorg. Chem.* **1976**, *15*, 2612–2615.
- [16]. Yu, S. B.; Holm, R. H. Aspects of the oxygen atom transfer chemistry of tungsten. *Inorg. Chem.* **1989**, *28*, 4385–4391.
- [17]. Vogel, A. I.; Jeffrey, G. H.; Bassett, J.; Mendam, J.; Denney, R. C. *Vogel's Textbook of Quantitative Chemical Analysis*; 5th ed.; Longman Higher Education: Harlow, England, 1999.
- [18]. Gross, D. C.; DeVay, J. E. Production and purification of syringomycin, a phytotoxin produced by *Pseudomonas syringae*. *Physiol. Plant Pathol.* **1977**, *11*, 13–28.
- [19]. Jain, P.; Kumar, D.; Chandra, S.; Misra, N. Experimental and theoretical studies of Mn(II) and Co(II) metal complexes of a tridentate Schiff's base ligand and their biological activities. *Appl. Organomet. Chem.* **2020**, *34*, e5371.
- [20]. Maurya, M. R.; Dhaka, S.; Avecilla, F. Synthesis, characterization, reactivity and catalytic activity of dioxidomolybdenum(VI) complexes derived from tribasic ONS donor ligands. *Polyhedron* **2014**, *81*, 154–167.
- [21]. Nishat, N.; Hasnain, S.; Dhyani, S.; Asma Coordination polymers of glutaraldehyde with glycine metal complexes: synthesis, spectral characterization, and their biological evaluation. *J. Coord. Chem.* **2010**, *63*, 3859–3870.
- [22]. Synthesis and characterization of homobinuclear complexes of UO₂(VI), Th(IV), ZrO(IV) and VO(IV) with Schiff-base monohydrazone derivatives. *J. Korean Chem. Soc.* **2008**, *52*, 468–475.
- [23]. Maurya, M. R.; Sarkar, B.; Avecilla, F.; Correia, I. Vanadium complexes derived from acetyl pyrazolone and hydrazides: Structure, reactivity, peroxidase mimicry and efficient catalytic activity for the oxidation of 1-phenylethanol. *Eur. J. Inorg. Chem.* **2016**, *2016*, 4028–4044.
- [24]. Zou, Y.; Liu, W.-L.; Xie, J.-L.; Ni, C.-L.; Ni, Z.-P.; Li, Y.-Z.; Meng, Q.-J.; Yao, Y.-G. Synthesis and crystal structure of metal complexes of Schiff bases derived from Glycylglycine and Salicylaldehyde [Ni(H₂O)₆(M)]₂·nH₂O (M = Cu, Ni; L = C₁₁H₉N₂O₄). *J. Coord. Chem.* **2004**, *57*, 381–391.
- [25]. Sharma, R. P.; Sharma, R.; Bala, R.; Quiros, M.; Salas, J. M. Synthesis, spectroscopic and X-ray structural study of cis-diazidobis(ethylenediamine)cobalt(III) thiocyanate. *J. Coord. Chem.* **2003**, *56*, 1581–1586.
- [26]. Ibrahim, K. M.; Gabr, I. M.; Zaky, R. R. Synthesis and magnetic, spectral and thermal eukaryotic DNA studies of some 2-acetylpyridine- [N-(3-hydroxy-2-naphthoyl)] hydrazone complexes. *J. Coord. Chem.* **2009**, *62*, 1100–1111.
- [27]. McGlynn, S. P.; Smith, J. K. The electronic structure, spectra, and magnetic properties of actinyl ions. *J. Mol. Spectrosc.* **1961**, *6*, 164–187.
- [28]. Jones, L. H. Determination of U-O bond distance in uranyl complexes from their infrared spectra. *Spectrochim. Acta* **1959**, *15*, 409–411.
- [29]. Maurya, M. R.; Kumar, M.; Kumar, A.; Costa Pessoa, J. Oxidation of p-chlorotoluene and cyclohexene catalysed by polymer-anchored oxovanadium(IV) and copper(II) complexes of amino acid derived tridentate ligands. *Dalton Trans.* **2008**, 4220–4232.
- [30]. Maurya, R. C.; Singh, H.; Pandey, A.; Singh, T. Metal chelates of bioinorganic and catalytic relevance: Synthesis, magnetic and spectral studies of some mononuclear and binuclear oxovanadium(IV) and dioxotungsten(VI) complexes involving Schiff bases derived from 4-butyl-3-methyl-1-phenyl-2-pyrazolin-5-one and certain aromatic amines. *Indian J. Chem. A* **2001**, *40*, 1053–1063.
- [31]. Mohanan, K.; Aswathy, R.; Nitha, L. P.; Mathews, N. E.; Kumari, B. S. Synthesis, spectroscopic characterization, DNA cleavage and antibacterial studies of a novel tridentate Schiff base and some lanthanide(III) complexes. *J. Rare Earths* **2014**, *32*, 379–388.
- [32]. Mondal, B.; Ghosh, T.; Sutradhar, M.; Mukherjee, G.; Drew, M. G. B.; Ghosh, T. Synthesis, structure and solution chemistry of a family of dinuclear hydrazone-vanadium(V) complexes with [OV(μ-O)VO]₄ core. *Polyhedron* **2008**, *27*, 2193–2201.
- [33]. Anantha Lakshmi, P. V.; Sariitha Reddy, P.; Jayatyaga Raju, V. Synthesis and structural studies of first row transition metal complexes of N-(2-nitro)-benzylidene-3-hydrazino quinoxaline-2-one. *Bull. Chem. Soc. Ethiop.* **2008**, *22* (3), 385–390.
- [34]. Özdemir, Ü. Ö.; Akkaya, N.; Özbek, N. New nickel(II), palladium(II), platinum(II) complexes with aromatic methanesulfonylhydrazone based ligands. Synthesis, spectroscopic characterization and in vitro antibacterial evaluation. *Inorganica Chim. Acta* **2013**, *400*, 13–19.
- [35]. Chitrapriya, N.; Mahalingam, V.; Zeller, M.; Natarajan, K. Synthesis, characterization, crystal structures and DNA binding studies of nickel(II) hydrazone complexes. *Inorganica Chim. Acta* **2010**, *363*, 3685–3693.
- [36]. Zaky, R. R.; Yousef, T. A. Spectral, magnetic, thermal, molecular modelling, ESR studies and antimicrobial activity of (E)-3-(2-(2-hydroxybenzylidene)hydrazinyl)-3-oxo-n(thiazole-2-yl)propanamide complexes. *J. Mol. Struct.* **2011**, *1002*, 76–85.
- [37]. Anaconda, J. R.; Rincones, M. Tridentate hydrazone metal complexes derived from cephalixin and 2-hydrazinopyridine: Synthesis, characterization and antibacterial activity. *Spectrochim. Acta A Mol. Biomol. Spectrosc.* **2015**, *141*, 169–175.
- [38]. Revanasiddappa, M.; Suresh, T.; Khasim, S.; Raghavendray, S. C.; Basavaraja, C.; Angadi, S. D. Transition Metal Complexes of 1,4(2'-Hydroxyphenyl-1-yl) di-imino azine: Synthesis, Characterization and Antimicrobial Studies. *E-J. Chem.* **2008**, *5*, 395–403.
- [39]. EL-Tabl, A. S.; EL-Saied, F. A.; AL-Hakimi, A. N. Synthesis, spectroscopic investigation and biological activity of metal complexes with ONO trifunctionalized hydrazone ligand. *Transit. Met. Chem.* **2007**, *32*, 689–701.
- [40]. Thaker, B. T.; Surati, K. R.; Oswal, S.; Jadeja, R. N.; Gupta, V. K. Synthesis, spectral, thermal and crystallographic investigations on oxo vanadium(IV) and manganese(III) complexes derived from heterocyclic β-diketone and 2-amino ethanol. *Struct. Chem.* **2007**, *18*, 295–310.
- [41]. Chiang Mai Journal of Science; Faculty of Science; Chiang Mai University Chiang Mai Journal of Science **2008**, *35* (3), 483–494. <https://epg.science.cmu.ac.th/ejournal/journal-detail.php?id=275> (accessed February 10, 2022).
- [42]. Saleem, M.; Sharma, M.; Sheikh, H. N.; Kalsotra, B. L. Synthesis and characterization of dinuclear molybdenum(VI) peroxo complexes with aryl hydrazones. *Ind. J. Chem. A* **2007**, *43*, 1423–1426.
- [43]. Kivelson, D.; Neiman, R. ESR studies on the bonding in copper complexes. *J. Chem. Phys.* **1961**, *35*, 149–155.
- [44]. Abdel-Rahman, L. H.; Abu-Dief, A. M.; El-Khatib, R. M.; Abdel-Fatah, S. M. Some new nano-sized Fe(II), Cd(II) and Zn(II) Schiff base complexes as precursor for metal oxides: Sonochemical synthesis, characterization, DNA interaction, in vitro antimicrobial and anticancer activities. *Bioorg. Chem.* **2016**, *69*, 140–152.
- [45]. Hanson, G. R.; Kabanos, T. A.; Keramidis, A. D.; Mentzafos, D.; Terzis, A. Oxovanadium(IV)-amide binding. Synthetic, structural, and physical studies of N-[2-(4-oxopent-2-en-2-ylamino)phenyl]pyridine-2-carboxamidooxovanadium(IV) and N-[2-(4-phenyl-4-oxobut-2-en-2-ylamino)phenyl]pyridine-2-carboxamidooxovanadium(IV). *Inorg. Chem.* **1992**, *31*, 2587–2594.
- [46]. Warren, B. E. *X-Ray Diffraction*; Dover Publications: Mineola, NY, 1990.
- [47]. Dianu, M. L.; Kriza, A.; Musuc, A. M. Synthesis, spectral characterization, and thermal behavior of mononuclear Cu(II), Co(II), Ni(II), Mn(II), and Zn(II) complexes with 5-bromosalicylaldehyde isonicotinoylhydrazone. *J. Therm. Anal. Calorim.* **2013**, *112*, 585–593.
- [48]. Coats, A. W.; Redfern, J. P. Kinetic parameters from thermogravimetric data. *Nature* **1964**, *201*, 68–69.
- [49]. Frost, A.; Pearson, R. Kinetics and mechanism, second edition. *J. Phys. Chem.* **1961**, *65*, 384–384.
- [50]. Narang, K. K.; Singh, K. B.; Singh, M. K.; Goyle, M. R.; Bhuvaneshwari, K.; Singh, V. Synthesis, characterization, dehydration, solid state conductance and biological activity of chromium(III) benzoyl hydrazin E azide/ sulphate complexes. *Synth. React. Inorg. Met.-Org. Nano-Met. Chem.* **1993**, *23*, 1313–1333.
- [51]. Wahed, M. G.; Bayoumi, H. A.; Mohamme, M. I. Physical properties of some acetylbenzaldehydehydrazone metal complexes. *Bull. Korean Chem. Soc.* **2003**, *24*, 1313–1318.

- [52]. Chohan, Z. H.; Pervez, H.; Rauf, A.; Khan, K. M.; Supuran, C. T. Isatin-derived antibacterial and antifungal compounds and their transition metal complexes. *J. Enzyme Inhib. Med. Chem.* **2004**, *19*, 417–423.
- [53]. Aljahdali, M. S.; El-Sherif, A. A.; Hilal, R. H.; Abdel-Karim, A. T. Mixed bivalent transition metal complexes of 1,10-phenanthroline and 2-aminomethylthiophenyl-4-bromosalicylaldehyde Schiff base: Spectroscopic, molecular modeling and biological activities. *Eur. J. Chem.* **2013**, *4*, 370–378.
- [54]. Tyagi, P.; Chandra, S.; Saraswat, B. S. Ni(II) and Zn(II) complexes of 2-((thiophen-2-ylmethylene)amino)benzamide: Synthesis, spectroscopic characterization, thermal, DFT and anticancer activities. *Spectrochim. Acta A Mol. Biomol. Spectrosc.* **2015**, *134*, 200–209.
- [55]. Phaniband, M. A.; Dhumwad, S. D. Synthesis, characterization and biological studies of CoII, NiII, CuII and ZnII complexes of Schiff bases derived from 4-substituted carbostyrils[quinolin2(1H)-ones]. *Transit. Met. Chem.* **2007**, *32*, 1117–1125.



Copyright © 2022 by Authors. This work is published and licensed by Atlanta Publishing House LLC, Atlanta, GA, USA. The full terms of this license are available at <http://www.eurjchem.com/index.php/eurjchem/pages/view/terms> and incorporate the Creative Commons Attribution-Non Commercial (CC BY NC) (International, v4.0) License (<http://creativecommons.org/licenses/by-nc/4.0>). By accessing the work, you hereby accept the Terms. This is an open access article distributed under the terms and conditions of the CC BY NC License, which permits unrestricted non-commercial use, distribution, and reproduction in any medium, provided the original work is properly cited without any further permission from Atlanta Publishing House LLC (European Journal of Chemistry). No use, distribution or reproduction is permitted which does not comply with these terms. Permissions for commercial use of this work beyond the scope of the License (<http://www.eurjchem.com/index.php/eurjchem/pages/view/terms>) are administered by Atlanta Publishing House LLC (European Journal of Chemistry).